Wideband MIMO Radar Waveform Design with Low Peak-to-Average Ratio Constraint

Yonghao Tang, Yimin D. Zhang, Moeness G. Amin, and Weixing Sheng

Abstract

Multiple-input multiple-output (MIMO) radar systems allow array antennas to transmit different waveforms and enable flexible transmit beampattern synthesis. Most existing transmit beampattern synthesis methods focus on narrowband MIMO radar system configurations. In this paper, we propose a novel technique to design transmit waveforms for wideband MIMO radar systems. This technique is based on the optimization of the cross-spectral density matrix and achieves a low peak-to-average power ratio as desired in practical radar systems. Simulation results are provided to verify the low PAR waveform design capability corresponding to arbitrary beampatterns.

Index Terms

Wideband MIMO radar, transmit beampattern synthesis, waveform design, peak-to-average power ratio.

I. Introduction

Multiple-input multiple-output (MIMO) radar is an emerging field that has attracted increasing interests [2–5]. Compared to conventional phased-array radar, one of the major advantages of

Part of the results was accepted for presentation at the 2015 IEEE China Summit and International Conference on Signal and Information Processing [1].

Y. Tang and W. Sheng are with the School of Electronic and Optical Engineering, Nanjing University of Science and Technology, Nanjing, Jiangsu, China.

Y. D. Zhang was with the Center for Advanced Communications, College of Engineering, Villanova University, USA. He is now with the Department of Electrical and Computer Engineering, College of Engineering, Temple University, Philadelphia, PA, USA.

M. G. Amin is with the Center for Advanced Communications, College of Engineering, Villanova University, Villanova, PA, USA.

MIMO radar is its waveform diversity that enables synthesis of transmit beampatterns with great flexibility [6]. Optimized MIMO radar waveform design plays a key role in achieving the desired system performance. Existing literature on MIMO radar waveform design focuses on narrowband signals [7–14] which can be generally classified into two main categories with different design objectives. The methods in the first category, including beampattern matching design and minimum sidelobe design, optimize the cross-correlation matrix of the transmit waveforms so as to achieve or closely approximate a desired transmit beampattern [6, 8, 9]. As the transmit beampattern is a linear function of the correlation matrix, optimized cross-correlation leads to desirable beampatterns. On the other hand, the objective of the methods in the second category is designing the actual transmit waveforms based on a given cross-correlation matrix. In [11, 14], for example, partially correlated signal design methods have been developed based on a given cross-correlation matrix for transmit energy concentration in an angular sector. Subarray- or subaperture-based waveform design methods trade off between coherent array directivity gain and diversity gain [7, 15]. By designing the waveforms to be coherent within each subarray but orthogonal across the different subarrays, these methods benefit from both types of gains. These design categories represent two-stage waveform design approaches, with the cross-correlation matrix acting as an intermediate result. Unfortunately, such approaches cannot be directly applied in the waveform design for wideband MIMO radars [16]. This is attributed to the fact that the cross-correlation matrix for wideband signals is not only a function of the array sensors but also of the time delays. As such, the problem is much more complicated than the narrowband case.

Compared to the narrowband MIMO radar, transmit beampattern synthesis for wideband MIMO radar systems has not received sufficient attention [16–18]. Inspired by the methods developed for narrowband MIMO radar systems, wideband transmit beampattern synthesis through optimizing the cross-spectral density matrix (CSDM) was first proposed in [16]. CSDM-based beampattern design performs independent cross-correlation matrix optimization in each frequency, thereby avoiding the consideration of convolutive time delays and achieving a flexible beampattern design with a low complexity. Beampattern matching design and minimum sidelobe design are examples of such beampattern design methods based on CSDM optimization for wideband MIMO radar [16, 17]. In these approaches, convex optimization techniques are used to generate the desired spatial beampatterns subject to transmit power constraints. Once the optimized CSDM is obtained, the next stage is to design the actual transmit waveforms according to

the optimized results. For example, the spectral density focusing beampattern synthesis technique (SFBT) [18] designs actual transmit waveforms based on the optimized CSDM. A major problem with these methods is that, because the waveforms at different frequencies are independently designed, the peak-to-average ratio (PAR) of synthesized waveforms across the array sensors is generally high. MIMO radars exploiting high PAR waveforms suffer from reduced radiation efficiency and signal distortion, and cause problems like harmonic interferences, reduction of power efficiency, and, for some systems, damages to transmitter equipment. Therefore, low PAR waveforms are highly desirable in practice, particularly when the transmit power is high.

Different from the CSDM-based waveform design methods, the wideband beampattern formation via iterative techniques (WBFIT) directly links the beampattern to signals through their Fourier transform [19], and the fast one-dimensional frequency invariant wideband transmit beampattern (F1D-FIWTB) method [20] designs waveforms through the Fourier transform by using frequency invariant beamforming (FIB) method developed in [21]. Although these methods can achieve low PAR waveforms with a desirable beampattern, they only solve simple beampattern matching design problems. As these methods do not utilize CSDM optimization, they cannot accommodate other constraints, such as low sidelobe beampattern or frequency-dependent beampatterns.

In this paper, we propose a novel two-stage technique for low PAR waveform design in the wideband MIMO radar context. The proposed technique is based on CSDM optimization and implements low PAR constraints in the waveform synthesis stage. In the first stage, CSDM optimization using convex optimization achieves the desired beampatterns satisfying mainlobe and sidelobe constraints. In the second stage, the proposed approach obtains low PAR waveforms based on the optimized CSDM. The key contribution of this paper lies in the development of a novel low PAR waveform design method based on the optimized CSDM. The proposed technique also supports waveforms design that synthesizes beampatterns with other desired constraints, such as low sidelobe levels.

The remainder of the paper is organized as follows. The signal model is formulated in Section II. In Section III, we summarize three beampattern design methods that optimize transmit beampatterns based on CSDM. Then, the proposed waveform design algorithm for CSDM-based wideband beampattern synthesis is presented in Section IV. Simulation results are provided in Section V to verify the effectiveness of the proposed technique. Conclusions are drawn in Section

VI.

Notations: We use lower-case (upper-case) bold characters to denote vectors (matrices). $(\cdot)^*$ denotes complex conjugate, and $(\cdot)^T$ and $(\cdot)^H$, respectively, denote transpose and conjugate transpose of a matrix or vector. trace$(\cdot)$ denotes the matrix trace, and diag$(\mathbf{x})$ denotes a diagonal matrix that uses the elements of $\mathbf{x}$ as its diagonal elements. $\mathbf{A} \succeq 0$ means that $\mathbf{A}$ is a positive semi-definite matrix. In addition, E$(\cdot)$ denotes statistical expectation, and Re$(\cdot)$ denotes the real part of a complex value. $||\cdot||_F$ denotes the Frobenius norm of a matrix.

II. SIGNAL MODEL

Consider a uniform linear array (ULA) consisting of M omnidirectional antennas with an inter-element spacing d. Denote the signal transmitted by the mth antenna as $s_m(t) = \mathrm{Re}\{x_m(t)e^{j2\pi f_c t}\}$, $m = 1, \ldots, M$, where f_c is the carrier frequency and $x_m(t)$ is the complex baseband waveforms occupying the spectral band $[-B/2, B/2]$. The received signal at a far-field point in the direction of θ can be expressed as

$$\hat{s}(t,\theta) = \sum_{m=1}^{M} s_m(t - \tau_m(\theta)), \tag{1}$$

where $\tau_m(\theta)$ denotes the time delay between the mth antenna and the reference one corresponding to the direction of θ. For notational simplicity, we use τ_m instead of $\tau_m(\theta)$ in the sequel. Then, the total signal power due to all signals is given by [16]

$$\begin{aligned}
\mathrm{E}\left\{\|\hat{s}(t,\theta)\|^2\right\} &= \mathrm{E}\left[\left\|\sum_{i=1}^{M} s_i^2(t) + \sum_{j,i=1,i\neq j}^{M} s_j(t-\tau_j)s_i(t-\tau_i)\right\|\right] \\
&= \sum_{i=1}^{M}\sum_{j=1}^{M} R_{ij}(\tau_i - \tau_j),
\end{aligned} \tag{2}$$

where

$$\begin{aligned}
R_{ij}(\tau_i - \tau_j) &= \mathrm{E}[s_i(t-\tau_i)s_j(t-\tau_j)] \\
&= \mathrm{E}\{\mathrm{Re}[x_i(t-\tau_i)e^{j2\pi f_c(t-\tau_i)}]\mathrm{Re}[x_j(t-\tau_j)e^{j2\pi f_c(t-\tau_j)}]\} \\
&= \frac{1}{2}\mathrm{Re}\{\bar{R}_{ij}(\tau_i - \tau_j)e^{-j2\pi f_c(\tau_i-\tau_j)}\},
\end{aligned} \tag{3}$$

with

$$\bar{R}_{ij}(\tau_i - \tau_j) = \frac{1}{2}\mathrm{E}\{x_i(t)x_j^*(t+\tau_i-\tau_j)\}. \tag{4}$$

For the assumed ULA, the power due to all transmitted signals at spatial angle θ can be represented as

$$P(\theta) = \mathrm{E}\left\{\|\hat{s}(t)\|^2\right\} = \frac{1}{2}\mathrm{Re}\left\{\sum_{i=1}^{M}\sum_{j=1}^{M}\bar{R}_{ij}(\tau_{ij})e^{j2\pi f_c\tau_{ij}}\right\}, \tag{5}$$

where $\tau_{ij} = \tau_i - \tau_j$.

For narrowband signals, only the carrier frequency f_c is considered. Because $\bar{R}_{ij}(\tau) \approx \bar{R}_{ij}(0)$, the spatial power distribution becomes [6]

$$P(\theta, f_c) = \boldsymbol{a}^H(\theta, f_c)\boldsymbol{R}\boldsymbol{a}(\theta, f_c), \tag{6}$$

where $\boldsymbol{R}$ is the narrowband signal cross-correlation matrix which can be properly chosen to synthesize the desired transmit beampattern [5, 6, 11], and $\boldsymbol{a}(\theta, f_c)$ is the narrowband array steering vector, which is defined as

$$\boldsymbol{a}(\theta, f_c) = [1 \;\; e^{j2\pi f_c d\cos\theta/l} \;\; \ldots \;\; e^{j2\pi f_c(M-1)d\cos\theta/l}]^T, \tag{7}$$

with l representing the velocity of electromagnetic wave propagation. The narrowband transmit waveforms that satisfy the cross-correlation matrix $\boldsymbol{R}$ can be designed using methods proposed in, e.g., [13, 14].

In the wideband case, the spatial power distribution is frequency-dependent over the frequency band $[f_c - B/2, f_c + B/2]$. We define the cross-spectral power density matrix (CSDM) at frequency f as [16],

$$\boldsymbol{S}(f) = \int \bar{\boldsymbol{R}}(\tau)e^{-2\pi f\tau}d\tau, \tag{8}$$

where the correlation matrix is given by

$$\bar{\boldsymbol{R}}(\tau) = \begin{bmatrix} \bar{R}_{11}(\tau) & \bar{R}_{12}(\tau) & \cdots & \bar{R}_{1M}(\tau) \\ \bar{R}_{21}(\tau) & \bar{R}_{22}(\tau) & \cdots & \bar{R}_{2M}(\tau) \\ \vdots & \vdots & \ddots & \vdots \\ \bar{R}_{M1}(\tau) & \bar{R}_{M2}(\tau) & \cdots & \bar{R}_{MM}(\tau) \end{bmatrix}. \tag{9}$$

The corresponding transmit power pattern is expressed as

$$P(\theta) = \int_{-B/2}^{B/2}\boldsymbol{a}^H(\theta, f_c + f)\boldsymbol{S}(f)\boldsymbol{a}(\theta, f_c + f)df, \tag{10}$$

where $\boldsymbol{a}(\theta, f_c + f)$ is the frequency-dependent array steering vector at frequency $f_c + f$, which is similarly defined as that in Eq. (7) by replacing the fixed frequency f_c by $f_c + f$, which varies

within the signal bandwidth. Divide the spectral range $[f_c - B/2, f_c + B/2]$ into N frequency bins, denoted as $f_{-N/2}$, $f_{-N/2+1}$, ..., $f_{N/2-1}$, where, without loss of generality, N is assumed to be even. The spatial angle interval $[-\pi/2, \pi/2]$ is divided into a K-point grid with the kth entry denoted as $\theta_k, k = 1, \ldots, K$. The power distribution at spatial angle θ_k and frequency f_n can then be written as

$$p(\theta_k, f_n) = \boldsymbol{a}^H(\theta_k, f_n)\boldsymbol{S}(f_n)\boldsymbol{a}(\theta_k, f_n). \tag{11}$$

From Eq. (11), it is clear that, at each frequency bin f_n, we can appropriately choose the CSDM $\boldsymbol{S}(f_n)$ to design the transmit beampattern in a similar manner to the narrowband case.

Note that large values of N and K enable a small mismatch error between the designed and the desired beampatterns. They require a long waveform and a high number of frequency grids, thus demanding a high computational complexity. On the contrarily, small values of these parameters may yield an unacceptable mismatch error. As such, it is important to choose the proper values of N and K that provide an acceptable mismatch error with an affordable computational complexity.

III. CSDM based Beampattern Optimization

As discussed in the previous section, the transmit beampattern of a ULA MIMO radar can be expressed using an integral expression in terms of CSDM $\boldsymbol{S}(f_n)$. Similar to the cross-correlation matrix in the narrowband case, the CSDM can be designed to optimally approximate a desired transmit beampattern in each frequency bin. In this section, effective methods for CSDM-based wideband beampattern design are introduced. We first summarize the beampattern matching design [16] and the minimum sidelobe beampattern design [17] methods. The min-max sidelobe beampattern design method, which is developed in [22] for narrowband waveform design, is then extended to wideband beampattern design. Among these methods, the beampattern matching design is useful when a specific beam shape is desired as this method achieves a desired beampattern through the optimization of the CSDM. On the other hand, the minimum sidelobe beampattern design yields a low sidelobe level, and the min-max sidelobe beampattern design provides flatter sidelobes in the synthesized beampattern. As such, the latter two methods are useful in applications where the sidelobe levels are mainly concerned. It is noted that, similar to the narrowband case, the CSDM determines the beampattern but does not directly lead to the actual transmitted waveform. In addition, because a wideband waveform synthesized from

multiple independently designed narrowband constant modulus waveforms is no longer constant modulus, separately designing narrowband waveforms at multiple subbands renders a high PAR in the yielding wideband waveform, which is undesirable in practice. The waveform design under low PAR constraints will be discussed in the next section.

A. Beampattern matching design

Similar to the narrowband MIMO radar beampattern design described in [9], the wideband beampattern of MIMO radar can also be designed by optimizing the CSDM $\boldsymbol{S}(f_n)$ to match a desired beampattern [16]. For a given desired beampattern $p_D(\theta_k, f_n)$, the CSDM $\boldsymbol{S}(f_n)$ can be deigned to minimize the following convex optimization problem

$$\begin{aligned} \min_{\{\boldsymbol{S}(f_n)\}_{n=-N/2}^{N/2-1},\beta} & \sum_{n=-N/2}^{N/2-1} \sum_{k=1}^{K} \left[p_D(\theta_k, f_n) - \beta p(\theta_k, f_n)\right]^2 \\ \text{s.t.} \quad & p(\theta_k, f_n) = \boldsymbol{a}^H(\theta_k, f_n)\boldsymbol{S}(f_n)\boldsymbol{a}(\theta_k, f_n), \quad \forall n, \\ & \boldsymbol{S}(f_n) \succeq 0, \quad \forall n, \\ & \text{trace}\left[\boldsymbol{S}(f_n)\right] = 1, \quad \forall n, \end{aligned} \tag{12}$$

where β is an auxiliary scale variable. The last two constraints require a semi-definite CSDM and unit transmit energy at every discrete frequency. In this formulation, we can arbitrarily choose the desired beampattern $p_D(\theta_k, f_n)$ to be synthesized in a wideband MIMO radar.

B. Minimum sidelobe beampattern design

In some applications, the beampattern is required to satisfy strict sidelobe constraints. This can be achieved by optimizing the CSDM $\boldsymbol{S}(f_n)$ [17]. The minimum sidelobe beampattern design for a wideband MIMO radar can be cast as the following semi-definite programming (SDP)

problem

$$\begin{aligned}
\min_{\{\boldsymbol{S}(f_n)\}_{n=-N/2}^{N/2-1},q} \quad & -q \\
\text{s.t.} \quad & \boldsymbol{S}(f_n) \succeq 0, \ \forall n, \\
& \text{trace}\left[\boldsymbol{S}(f_n)\right] = 1, \ \forall n, \\
& \boldsymbol{a}^H(\theta_0, f_n)\boldsymbol{S}(f_n)\boldsymbol{a}(\theta_0, f_n) - \boldsymbol{a}^H(\theta_k, f_n)\boldsymbol{S}(f_n)\boldsymbol{a}(\theta_k, f_n) \geq q, \theta_k \in \boldsymbol{\Theta}, \ \forall n, \\
& \boldsymbol{a}^H(\theta_l, f_n)\boldsymbol{S}(f_n)\boldsymbol{a}(\theta_l, f_n) = \frac{1}{2}\boldsymbol{a}^H(\theta_0, f_n)\boldsymbol{S}(f_n)\boldsymbol{a}(\theta_0, f_n), \ \forall n, \\
& \boldsymbol{a}^H(\theta_r, f_n)\boldsymbol{S}(f_n)\boldsymbol{a}(\theta_r, f_n) = \frac{1}{2}\boldsymbol{a}^H(\theta_0, f_n)\boldsymbol{S}(f_n)\boldsymbol{a}(\theta_0, f_n), \ \forall n,
\end{aligned} \tag{13}$$

where q is an auxiliary variable, $\boldsymbol{\Theta}$ is the sidelobe regions, θ_0 represents the main beam direction, and θ_l and θ_r are the lower and upper angles determining the 3dB beam-width at each frequency. The main beam direction and beam-width are determined by properly choosing θ_0, θ_l and θ_r.

C. Min-max sidelobe beampattern design

Another sidelobe rejection constraint was proposed in [22] to obtain much flatter sidelobe levels than that provided by the minimum sidelobe beampattern design. This approach, referred to as min-max sidelobe beampattern design, can be modified for wideband MIMO radar beampattern design, expressed as

$$\begin{aligned}
\min_{\{\boldsymbol{S}(f_n)\}_{n=-N/2}^{N/2-1},q} \max_{\theta_k \in \boldsymbol{\Theta}} \ & p(\theta_k, f_n) \\
\text{s.t.} \quad & p(\theta_k, f_n) = \boldsymbol{a}^H(\theta_k, f_n)\boldsymbol{S}(f_n)\boldsymbol{a}(\theta_k, f_n), \ \forall n, \\
& \boldsymbol{S}(f_n) \succeq 0, \ \forall n, \\
& \text{trace}\left[\boldsymbol{S}(f_n)\right] = 1, \ \forall n, \\
& \boldsymbol{a}^H(\theta_l, f_n)\boldsymbol{S}(f_n)\boldsymbol{a}(\theta_l, f_n) = \frac{1}{2}\boldsymbol{a}^H(\theta_0, f_n)\boldsymbol{S}(f_n)\boldsymbol{a}(\theta_0, f_n), \ \forall n, \\
& \boldsymbol{a}^H(\theta_r, f_n)\boldsymbol{S}(f_n)\boldsymbol{a}(\theta_r, f_n) = \frac{1}{2}\boldsymbol{a}^H(\theta_0, f_n)\boldsymbol{S}(f_n)\boldsymbol{a}(\theta_0, f_n), \ \forall n.
\end{aligned} \tag{14}$$

This optimization problem is also convex and thus can be conveniently solved.

IV. LOW PAR WAVEFORMS DESIGN METHOD

In narrowband MIMO radar, transmit waveforms can be designed according to a given correlation matrix $\boldsymbol{R}$ [6, 8, 9]. For wideband MIMO radars, however, transmit waveform design based on the correlation function matrix $\bar{\boldsymbol{R}}(\tau)$ becomes more complicated as $\bar{\boldsymbol{R}}(\tau)$ involves different lags. To the best of our knowledge, low PAR waveform design based on the optimized CSDM has not been considered so far. In the following, we propose a novel approach to design low PAR waveforms that approximately satisfy a specified CSDM. The problem is first considered for the case where the CSDM is rank-one, and then a general case for a higher-rank CSDM is considered.

A. Single-rank Case

We first consider the simple case where the CSDM $\boldsymbol{S}(f_n)$ at each frequency has a single primary eigenvalue, whereas the other eigenvalues are negligible. In this case, $\boldsymbol{S}(f_n)$ can be expressed as

$$\boldsymbol{S}(f_n) = \boldsymbol{y}_n \boldsymbol{y}_n^H, \tag{15}$$

where $\boldsymbol{y}_n$ represents the primary eigenvector. Performing eigen-decomposition of $\boldsymbol{S}(f_n)$ for each frequency $f_n, n = -N/2, \ldots, N/2-1$, we express the transmit waveforms in the frequency domain as

$$\boldsymbol{Y} = [\boldsymbol{y}_{-N/2}, \boldsymbol{y}_{-N/2+1}, \ldots, \boldsymbol{y}_{N/2-1}] = [\tilde{\boldsymbol{y}}_1, \tilde{\boldsymbol{y}}_2, \ldots, \tilde{\boldsymbol{y}}_M]^T, \tag{16}$$

where $\tilde{\boldsymbol{y}}_m^T$ denotes the mth row of $\boldsymbol{Y}$, $m = 1, ..., M$. The N-symbol transmit sequence $\boldsymbol{x}_m$ corresponding to each $\tilde{\boldsymbol{y}}_m$ can then be computed through inverse discrete Fourier transform (IDFT).

As the waveform is independently optimized in each frequency, the yielding waveforms that combine all the frequency components will have a high PAR. Maintaining a low PAR is important in practice to minimize energy loss and signal distortions. For this purpose, the low PAR waveform design problem is described as

$$\begin{aligned} &\min_{\boldsymbol{X}, \boldsymbol{\phi}} \|\boldsymbol{Z} - \boldsymbol{X}\|_F \\ &\text{s.t.} \quad \text{PAR}(\boldsymbol{x}_m) \leq \rho, \ \forall m, \\ &\quad \|\boldsymbol{x}_m\|_2^2 = c, \ \forall m, \end{aligned} \tag{17}$$

where

$$\boldsymbol{Z} = [\tilde{\boldsymbol{z}}_1, \tilde{\boldsymbol{z}}_2, \ldots, \tilde{\boldsymbol{z}}_M]^T_{M\times N}, \tag{18}$$

$$\tilde{\boldsymbol{z}}_m = \text{IDFT}[\text{diag}(\boldsymbol{\phi})\tilde{\boldsymbol{y}}_m], \tag{19}$$

$$\boldsymbol{X} = [\boldsymbol{x}_1, \boldsymbol{x}_2, \ldots, \boldsymbol{x}_M]^T_{M\times N}, \tag{20}$$

IDFT$(\cdot)$ is the IDFT operator, and $\boldsymbol{\phi} = [\phi_{-N/2}, \ldots, \phi_{N/2-1}]$ represents the phase ambiguities because $\boldsymbol{S}(f_n)$ is transparent to the signal group phase, i.e., $\boldsymbol{y}_n\phi_n\phi_n^*\boldsymbol{y}_n^H = \boldsymbol{y}_n\boldsymbol{y}_n^H = \boldsymbol{S}(f_n)$. In addition, c is the energy transmitted from each transmitter, and $\rho \geq 1$ is the maximum permissible PAR of the mth sequence, defined as

$$\text{PAR}(\boldsymbol{x}_m) = \frac{N\max|\boldsymbol{x}_m(n)|^2}{\sum_n |\boldsymbol{x}_m(n)|^2}. \tag{21}$$

Note that $\rho = 1$ implies that the resulting waveform is constant-modulus.

Because of the complex expression (21), the minimization in (17) with respect to $\boldsymbol{X}$ and $\boldsymbol{\phi}$ does not have a closed-form solution. However, several local optimal solutions with respect to either $\boldsymbol{X}$ or $\boldsymbol{\phi}$ dimension are available. In the proposed iterative algorithm, this optimization problem is solved by iteratively updating the individual optimization problems with respect to the transmit waveforms $\boldsymbol{X}$ and the phase ambiguity $\boldsymbol{\phi}$. This kind of optimization techniques has been applied in, e.g., [23, 24] with a guaranteed convergence. The proposed iterative algorithm is summarized in Algorithm 1.

B. General Case

We now extend the proposed method to the general case where the rank of the CSDM $\boldsymbol{S}(f_n)$ is larger than one. In this case, $\boldsymbol{S}(f_n)$ is expressed as

$$\boldsymbol{S}(f_n) = \epsilon_{n_1}\boldsymbol{y}_{n_1}\boldsymbol{y}_{n_1}^H + \epsilon_{n_2}\boldsymbol{y}_{n_2}\boldsymbol{y}_{n_2}^H + \ldots + \epsilon_{n_D}\boldsymbol{y}_{n_D}\boldsymbol{y}_{n_D}^H, \tag{25}$$

where D is the number of the primary eigenvalues of $\boldsymbol{S}(f_n)$, and ϵ_{n_d} and $\boldsymbol{y}_{n_d}$ denote the dth largest eigenvalue and the corresponding eigenvector, respectively. Similar to the single-rank case as described in Section IV-A, each set of $\{\boldsymbol{y}_{n_d}\}_{n=-N/2}^{N/2-1}$ can be used to compute a set of $\{\boldsymbol{Y}_d, \boldsymbol{Z}_d, \boldsymbol{X}_d\}$, $d = 1, ..., D$.

Algorithm 1 Iterative algorithm for waveform design

1: Apply eigen-decomposition to the given $\boldsymbol{S}(f_n)$, and initialize $\boldsymbol{\phi} = [e^{j0}, \ldots, e^{j0}]$;

2: Compute $\boldsymbol{Y}$ and $\boldsymbol{Z}$ by Eqs. (16), (18), and (19);

3: For each $m, m = 1, \ldots, M$, solve the nearest-vector problems [25] to obtain x_m based on $\boldsymbol{\phi}$:

$$\begin{aligned} &\min_{\boldsymbol{x}_m} \|\tilde{\boldsymbol{z}}_m - \boldsymbol{x}_m\|_2 \\ &\text{s.t.} \quad \text{PAR}(\boldsymbol{x}_m) \leq \rho, \\ &\|\boldsymbol{x}_m\|_2^2 = c. \end{aligned} \tag{22}$$

4: For each $n, n = -N/2, \ldots, N/2 - 1$, update ϕ_n based on the estimated $\boldsymbol{X}$ by solving

$$\min_{\phi_n} \|\boldsymbol{y}_n \phi_n - \hat{\boldsymbol{y}}_n\|_2, \tag{23}$$

where $\hat{\boldsymbol{y}}_n$ is the nth column of [DFT($\boldsymbol{x}_1$), DFT($\boldsymbol{x}_2$),. . ., DFT($\boldsymbol{x}_M$)]^T, with DFT$(\cdot)$ representing the discrete Fourier transform (DFT) operator. This minimization problem (23) has a closed-form solution:

$$\phi_n = \exp\{j \arg[\boldsymbol{y}_n^H \hat{\boldsymbol{y}}_n]\}. \tag{24}$$

5: Repeat steps 2 to 4 until convergence is achieved.

It is noted that simultaneous transmission of the optimized waveforms $\boldsymbol{X}_d, d = 1, \ldots, D$, will violate the PAR constraints. As such, the D waveforms are sequentially transmitted, i.e., the transmit waveforms are expressed as

$$\hat{\boldsymbol{X}} = [\boldsymbol{X}_1, \boldsymbol{X}_2, \ldots, \boldsymbol{X}_D]_{M \times DN}. \tag{26}$$

Consequently, the low PAR waveform design problem in (17) can be modified as

$$\begin{aligned} &\min_{\hat{\boldsymbol{X}}, \boldsymbol{\phi}} \|\hat{\boldsymbol{Z}} - \hat{\boldsymbol{X}}\|_F \\ &\text{s.t.} \quad \text{PAR}(\hat{\boldsymbol{x}}_m) \leq \rho, \text{for each } m, \\ &\|\hat{\boldsymbol{x}}_m\|_2^2 = c, \text{for each } m, \end{aligned} \tag{27}$$

where $\hat{\boldsymbol{Z}} = [\boldsymbol{Z}_1, \boldsymbol{Z}_2, \ldots, \boldsymbol{Z}_D]_{M \times DN}$. The solution for the minimization problem in (27) follows the same iterative steps as in Algorithm 1.

Note that, as the D waveforms are sequentially transmitted, the overall waveforms span a longer time period as the number of significant eigenvalues increases. In practice, therefore, there is a tradeoff between the pulse width and the code width such that the total waveform length is acceptable.

C. Analysis

Unlike the WBFIT method [19], which only solves the beampattern matching problem, and the SFBT method [18], which does not design low PAR waveforms based on a given CSDM, the proposed algorithm can synthesize low PAR transmit waveforms which match any given CSDM corresponding to an arbitrary beampattern. The proposed method is generally suboptimal because there are distortions between the resulting beampattern and the desired one due to two factors. One is caused by the negligence of insignificant eigen-terms in Eqs. (15) and (25). This error can be controlled by properly choosing the number of effective eigenvalues of $\boldsymbol{S}(f_n)$. A large value of D generally yields a smaller error in (25), but will result in a longer transmit sequence. Note that each eigen-term requires a separate waveform to be cascaded, and the waveform magnitude is determined to meet the PAR requirement. Therefore, when a low PAR is required, the waveform corresponding to a small eigenvalue, which has to be transmitted with a similar power so as to meet the PAR requirement, yields overall beampattern distortion. Consequently, we should choose a minimum number of primary eigenvalues, D, such that their sum exceeds a certain percentage (say, 99%) of the sum of all eigenvalues, as suggested in [26]. On the other hand, a strict low PAR constraint also results in mismatches between the optimized and desired beampatterns, especially in multi-rank case. This can only be relieved by choosing a larger value of ρ within the acceptable limit.

The overall computational complexity of the proposed method is $\mathcal{O}(L_1KN(M^2I^{2.5}+I^3)+NM^3+L_2DMN(N+\log_2 N))$, where L_1 and L_2 are the numbers of iterations in each stage, and I is the number of the constraints. In comparison, the complexities of WBFIT in [19] and F1D-FIWTB in [20] are $\mathcal{O}(L_3(K+M)NM^2+L_4MN(N+\log_2 N))$ and $\mathcal{O}(M_1N\log_2 M_1+L_5MN(N+\log_2 N))$, respectively, where L_3, L_4, and L_5 are, respectively, the numbers of iterations in different stages, and $M_1 \geq M$. The computational complexity of the proposed method is similar to the WBFIT method, and is slightly higher than the F1D-FIWTB because the latter does not require iterations when computing the first term.

V. SIMULATION RESULTS

In this section, we provide simulation results to demonstrate the effectiveness of the proposed algorithm for wideband MIMO waveform design based on a given CSDM, which can be obtained by the optimization methods described in Section III. Throughout the simulations, the carrier frequency of the transmitted signals is $f_c = 1$ GHz. The signal bandwidth is set as $B = 100$ MHz, and $N = 64$ frequency-domain samples are used. The inter-element spacing is set as half wavelength at the highest in-band frequency to avoid grating lobes. In addition, the spatial region is divided into $K = 181$ grid points.

A. Performance comparison

In this example, the number of transmit antennas is set as M=16. The minimum sidelobe beampattern design method is adopted to design the desired beampattern pointing at 0° with a main beam width of 8°. The sidelobe regions are set as

$$\mathbf{\Theta} = [-90^\circ, -9^\circ] \cup [9^\circ, 90^\circ], -N/2 \leq n < N/2. \tag{28}$$

Note that buffer zones with a width of 5° are assumed between the -3 dB power points and the sidelobe regions. By solving the optimization problem (13), we obtain the CSDM $\boldsymbol{S}(f_n)$ at each frequency f_n. The desired beampattern computed from the optimized CSDM is shown in Fig. 1(a). In the proposed method, D is chosen to be 2, and the PAR constraint is set as $\rho = 2$. As shown in Fig. 1(b), the beampattern synthesized by the actual waveforms is very close to the desired one except small distortions in the sidelobe region. As shown in Fig. 2, when compared to the synthesized beampattern using the method introduced in [19], the proposed method achieves a lower sidelobe level as a result of the sidelobe constraint in the CSDM optimization, although the mainlobe beamwidth becomes slightly wider. However, such constrained problem cannot be solved by the method developed in [19].

B. Beampattern design with wide main beam

The rank of CSDM may increase with the increase of the width of main beam or the number of main beams. In this example, the beampattern matching method is adopted to design the transmit beampattern with a wide beam under the low PAR constraint. The ULA is assumed to

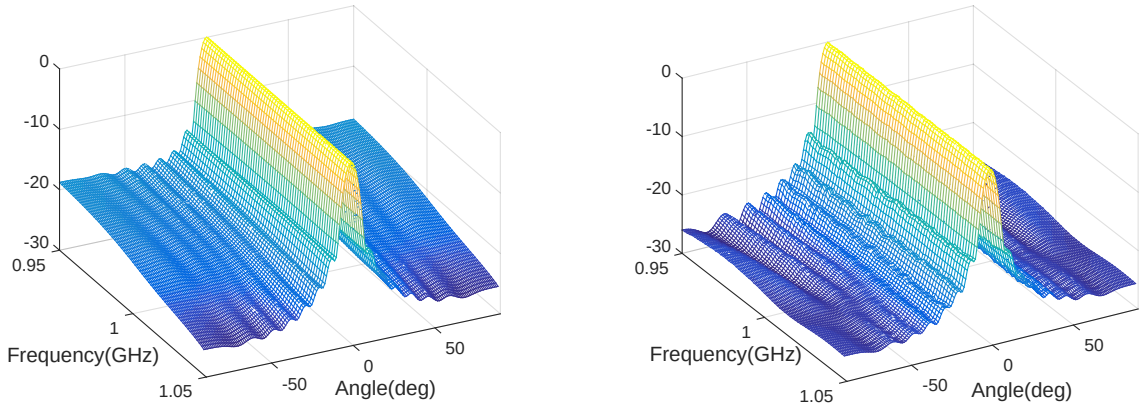

Fig. 1. Beampatterns synthesized with respect to spatial angle and frequency using (a) the optimized CSDM and (b) the proposed iterative algorithm with ρ=2.

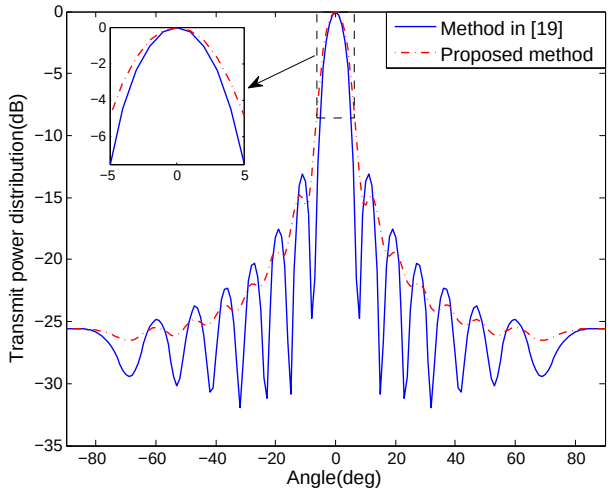

Fig. 2. Comparison of beampatterns generated by two different methods with respect to spatial angle dimension.

have $M = 10$ antennas. The desired beampattern is assumed as

$$p_D(\theta_k, f_n) = \begin{cases} 1, & -20^\circ \le \theta_k \le 20^\circ, \\ 0, & \text{otherwise}, \end{cases} \tag{29}$$

for all f_n. That is, the beampattern has a main beam pointing at 0° with a beam-width of 40° across the entire frequency band. The desired transmit beampattern in spatial angle-dimension is shown in Fig. 3. According to the optimized CSDM obtained by solving the problem in (12), a set of frequency-domain waveforms $\{\boldsymbol{Y}_1, \boldsymbol{Y}_2, \boldsymbol{Y}_3\}$ are generated, i.e., $D = 3$. The beampattern

synthesized by the optimized CSDM is shown in Fig. 4. By applying the proposed method in (27), the final extended transmit sequences can be obtained as $\hat{\boldsymbol{X}} = [\boldsymbol{X}_1, \boldsymbol{X}_2, \boldsymbol{X}_3]_{M\times 3N}$. We perform the proposed method under two different PAR constraints of $\rho = 1$ and $\rho = 2$, respectively. The corresponding beampatterns are shown in Fig. 5. The beampatterns with respect to the spatial angle computed from the optimized CSDM and the designed waveforms are also shown in Fig. 3 along with the desired one. It is evident from Fig. 5(a) that the transmit beampattern synthesized by the actual waveforms suffers distortions owing to the strict constant modulus ($\rho = 1$) constraint. By relaxing the constraint to $\rho = 2$, as shown in Fig. 5(b), the beampattern distortions become much less significant. As such, we would need to trade off the PAR constraint and acceptable beampattern distortions.

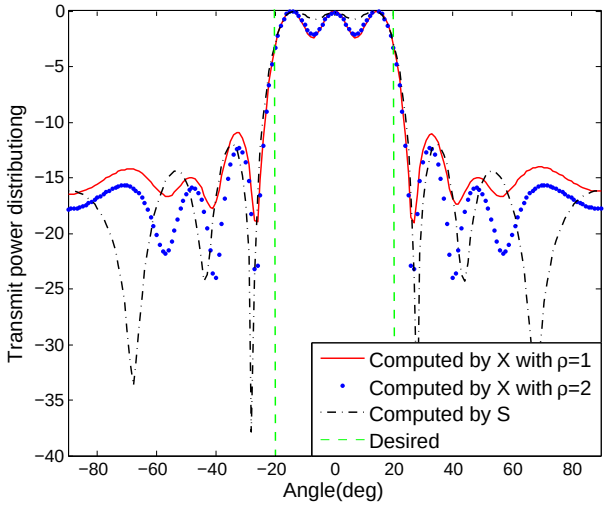

Fig. 3. Comparison of beampatterns generated by four different methods.

C. Beampattern design with multiple frequency subbands

In this experiment, the ULA is assumed to have M=12 antennas. As shown in Fig. 6, a beam pointing at 20° with a 10° beam-width is desired in one of the two equally divided subbands, whereas another beam, pointing at -30° with the same 10° beam-width, is desired in the other subband. In this case, the sidelobe regions are set as

$$\boldsymbol{\Theta} = \begin{cases} [-90^\circ, 10^\circ] \cup [30^\circ, 90^\circ], & -N/2 \le n < 0, \\ [-90^\circ, -40^\circ] \cup [-20^\circ, 90^\circ], & 0 \le n < N/2. \end{cases} \tag{30}$$

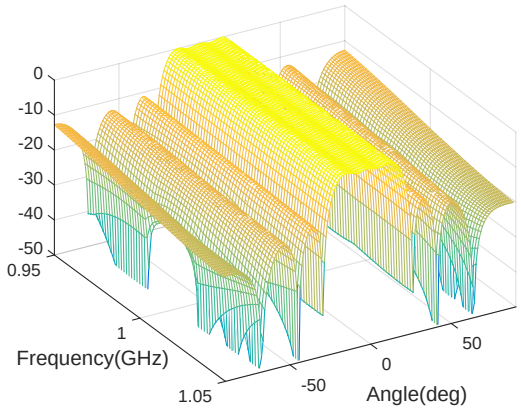

Fig. 4. Beampattern synthesized using the optimized $\boldsymbol{S}(f)$ with respect to spatial angle and frequency.

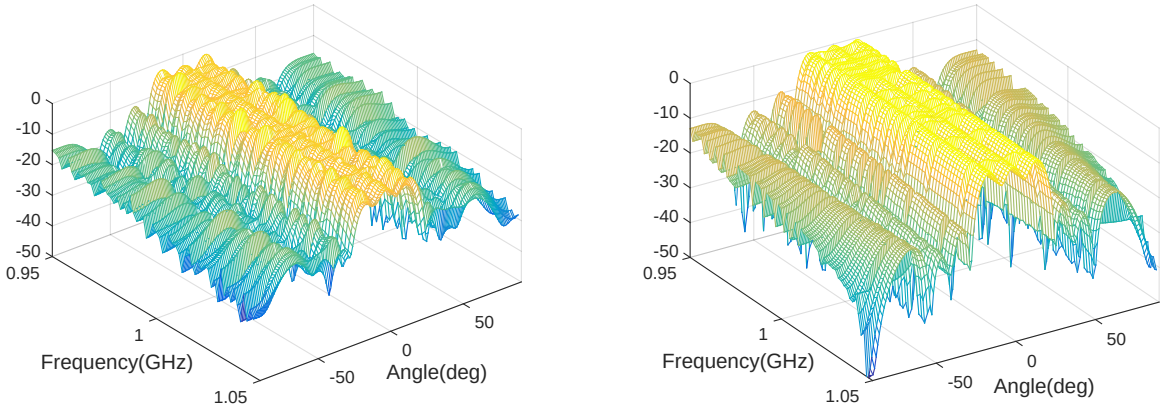

(a) (b)

Fig. 5. Beampatterns synthesized using the proposed method with respect to spatial angle and frequency: (a) ρ=1, (b) ρ=2.

The min-max sidelobe beampattern design in (14) is adopted to design the transmit beampattern, and the single-rank CSDM is obtained. Fig. 6 shows the beampattern synthesized from the optimized CSDM with respect to spatial angle and frequency. The transmit beampatterns synthesized by the actual waveforms under the constraints of ρ=1 and ρ=2 are respectively shown in Figs. 7(a) and 7(b). The comparison clearly shows that a higher PAR constraint allows the synthesized beampattern to be smoother and less distorted. As the CSDM at each frequency only has a single primary eigenvalue, the main beams suffer less distortion than the higher-rank case in Subsection V-B. It is also revealed that the transmit waveforms can be effectively

generated by the proposed method under a lower PAR or constant-modulus constraint with a tolerable distortion in the single-rank case.

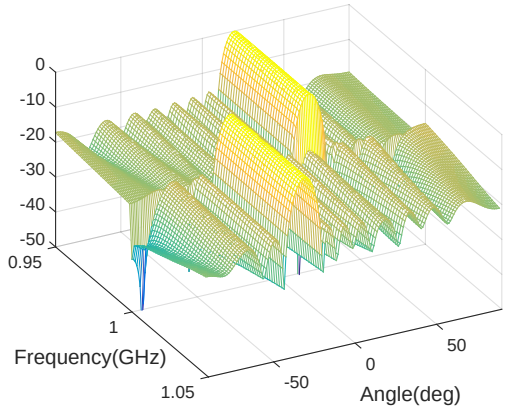

Fig. 6. Beampattern synthesized using the optimized CSDM with respect to spatial angle and frequency.

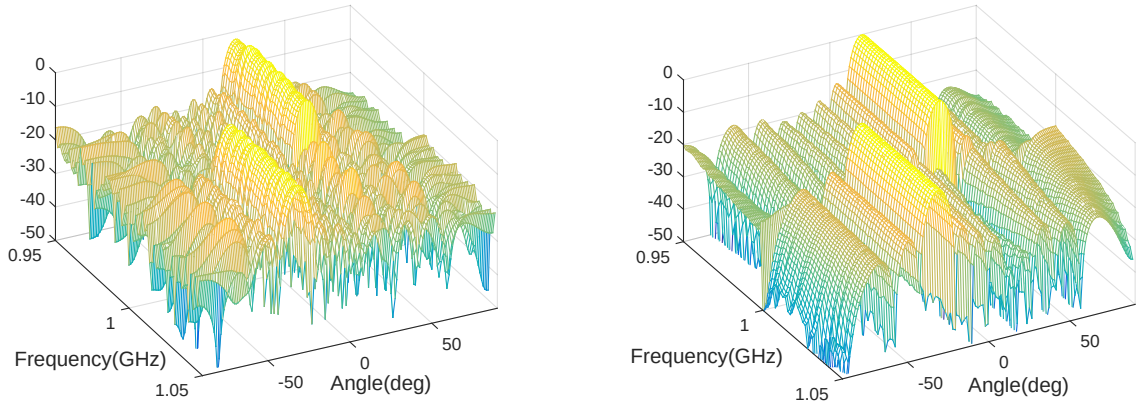

(a) (b)

Fig. 7. Beampatterns synthesized using the proposed method with respect to spatial angle and frequency: (a) ρ=1, (b) ρ=2.

D. Beampattern design under special constraints

In some applications, special transmit beampatterns are desired. For example, certain airborne radars require extreme low sidelobe in one side of the spatial angle regions in order to suppress ground clutter. Other applications require no transmission to be made to a spatial region to

avoid interference. Such constraints must be reflected in the waveform design. In this example, a beampattern with single-side extreme low sidelobe (less than -20 dB) is desired with a ULA of $M = 15$ antennas. The beampattern matching design in (12) is adopted, and the desired beampattern is assumed as

$$p_D(\theta_k, f_n) = \begin{cases} 1, & -5^\circ \le \theta_k \le 5^\circ, \\ 0, & \theta_k \in \boldsymbol{\Theta}, \end{cases} \tag{31}$$

for all f_n, where $\boldsymbol{\Theta} = [-90^\circ, -10^\circ]$, for all n. Note that in this example the sidelobe level in the other side is not of a concern because it does not cause undesired interference. In this case, the extra sidelobe constraint for the extreme low sidelobe requirement in the concerned single-side is set as

$$10\log_{10}(\boldsymbol{a}^H(\theta_j, f_n)\boldsymbol{S}(f_n)\boldsymbol{a}(\theta_j, f_n) - \boldsymbol{a}^H(\theta_0, f_n)\boldsymbol{S}(f_n)\boldsymbol{a}(\theta_0, f_n)) \le -30\text{dB}, \theta_k \in \boldsymbol{\Theta}. \tag{32}$$

The WBFIT [19] and F1D-FIWTB [20] approaches provide a closed-form solution to obtain the waveforms in the frequency domain in each iterative process. They are, however, effective only when the optimization is unconstrained and thus fail to solve this waveform design problem for the particular constraint described in (32). However, the approach proposed in this paper can obtain the CSDM corresponding to the desired beampattern by solving the optimization problem in (12) subject to the additional constraint (32). Applying the proposed waveform design algorithm to the optimized CSDM, the extended waveforms ($D = 2$) are obtained under a PAR constraint of $\rho = 2$. The beampatterns synthesized by the optimized CSDM and the actual waveforms are shown in Fig. 8 with respect to the spatial angle and frequency. Both requirements described in (31) and (32) are satisfied, and the distortion of the beampattern synthesized by the actual waveforms is insignificant and is confined within the sidelobe regions.

VI. CONCLUSION

In this paper, we proposed a novel optimization method to design transmit waveforms based on arbitrary cross-spectral density matrix (CSDM) for wideband multiple-input multiple-output (MIMO) radars. In particular, the proposed waveform design methods yield waveforms that satisfy low peak-to-average ratio (PAR) constraints while meeting the specified CSDM. The proposed techniques were successfully applied to handle both single-rank and multi-rank cases, and to support multiple frequency subband and single-side beampattern syntheses. Simulation

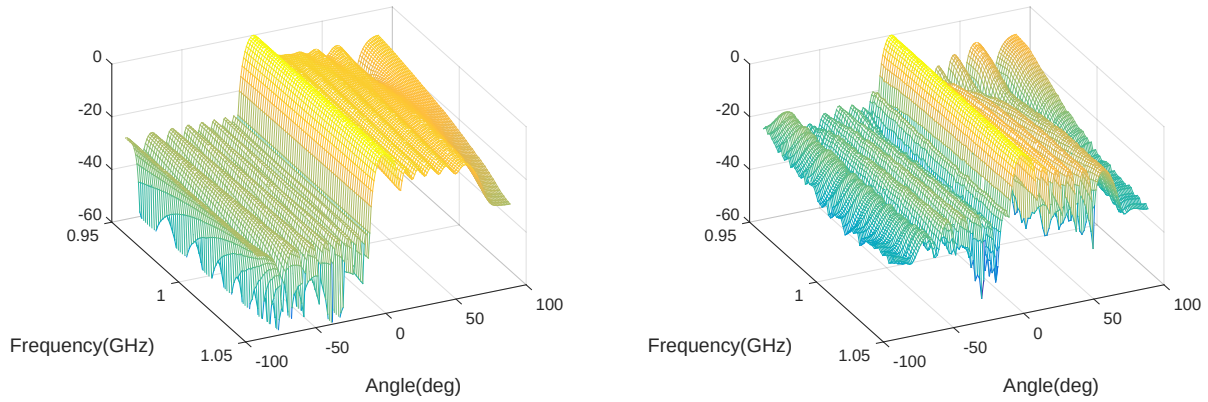

Fig. 8. Comparison of beampatterns with respect to spatial angle and frequency: (a) synthesized by optimized CSDM, (b) synthesized by actual waveforms with ρ=2.

results verified the effectiveness of the proposed algorithm for designing low PAR waveforms that synthesize the desired beampatterns.

ACKNOWLEDGMENT

The work of Y. Tang and W. Sheng was supported in part by the National Natural Science Foundation of China under Grant 11273017 and Grant 61471196.

REFERENCES

[1] Y. Tang, Y. D. Zhang, M. G. Amin, and W. Sheng, "Design of wideband MIMO radar wavforms low peak-to-average-power ratio," in *Proceedings of IEEE China Summit and International Conference on Signal and Information Processing*, 2015.

[2] E. Fishler, A. Haimovich, R. Blum, D. Chizhik, L. Cimini, and R. Valenzuela, "MIMO radar: An idea whose time has come," in *Proceedings of IEEE Radar Conference*, 2004, pp. 71–78.

[3] F. Daum and J. Huang, "MIMO radar: snake oil or good idea?," *IEEE Aerospace and Electronic Systems Magazine*, vol. 24, pp. 8–12, 2009.

[4] M. Haimovich, R. S. Blum, and L. J. Cimini, "MIMO radar with widely separated antennas," *IEEE Signal Processing Magazine*, vol. 25, pp. 116–129, 2008.

[5] J. Li and P. Stoica, "MIMO radar with co-located antenna: Review of some recent work," *IEEE Signal Processing Magazine*, vol. 24, pp. 106–114, 2007.

[6] D. R. Fuhrmann and G. San Antonio, "Transmit beamforming for MIMO radar systems using signal cross-correlation," *IEEE Transactions on Aerospace and Electronic Systems*, vol. 44, pp. 171–186, 2009.

[7] A. Hassanien and S. Vorobyov, "Phased-MIMO radar: A tradeoff between phased-array and MIMO radars," *IEEE Transactions on Signal Processing*, vol. 58, pp. 3137–3151, 2010.

[8] P. E. Berry and D. Yau, "Optimal fast-time beamforming with linearly independent waveforms," *Signal Processing*, vol. 89, pp. 492–501, 2009.

[9] J. Li, P. Stoica, and Y. Xie, "On probing signal design for MIMO radar," in *Proceedings of Asilomar Conference on Signals, Systems and Computers*, 2006, pp. 31–35.

[10] R. Boyer, "Co-located MIMO radar with orthogonal waveform coding : Cramer-Rao lower bound," in *Proceedings of IEEE International Workshop on Computational Advances in Multi-Sensor Adaptive Processing*, 2009, pp. 149–152.

[11] S. Ahmed, J. S. Thompson, and Y. Petillot, "Unconstrained synthesis of covariance matrix for MIMO radar transmit beampattern," *IEEE Transactions on Signal Processing*, vol. 59, pp. 3837–3849, 2011.

[12] J. Li, P. Stoica, K. Forsythe, and D. Bliss, "Range compression and waveform optimization for MIMO radar: A Cramer-Rao bound based study," *IEEE Transactions on Signal Processing*, vol. 56, pp. 218–232, 2008.

[13] P. Stoica, J. Li, and X. Zhu, "Waveform synthesis for diversity-based transmit beampattern design," *IEEE Transactions on Signal Processing*, vol. 56, pp. 2593–2598, 2008.

[14] S. Ahmed, J. S. Thompson, B. Mulgrew, and Y. Petillot, "Finite alphabet constant-envelope waveform design for MIMO radar," *IEEE Transactions on Signal Processing*, vol. 59, pp. 5326–5337, 2011.

[15] H. Li and B. Himed, "Transmit subaperturing for MIMO radars with co-located antennas," *IEEE Journal of Selected Topics in Signal Processing*, vol. 4, pp. 55–65, 2010.

[16] G. San Antonio and D. R. Fuhrmann, "Beampattern synthesis for wideband MIMO radar systems," in *Proceedings of IEEE International Workshop on Computational Advances in Multi-Sensor Adaptive Processing*, 2005, pp. 105–108.

[17] Y. Jin, X. Liu, and J. Huang, "Wideband transmit beampattern design for MIMO array," in *Proceedings of IEEE International Conference on Signal Processing, Communications and Computing*, 2011, pp. 1–4.

[18] P. Jardin, F. Nadal, and S. Middleton, "On wideband MIMO radar: Extended signal model and spectral beampattern design," in *Proceedings of European Radar Conference*, 2010, pp. 382–395.

[19] H. He, P. Stoica, and J. Li, "Wideband MIMO systems: signal design for transmit beampattern synthesis," *IEEE Transactions on Signal Processing*, vol. 59, pp. 618–628, 2011.

[20] T. Yang, S. Tao, and Z. Wu, "Fast frequency invariant transmit beampattern synthesis for wideband MIMO radar," in *Proceedings of IET International Conference on Radar Systems*, 2012, pp. 52–52.

[21] W. Liu and W. Stephan, "Design of frequency invariant beamformers for broadband arrays," *IEEE Transactions on Signal Processing*, vol. 56, pp. 855–860, 2008.

[22] X. Ma, Y. Tang, and W. Sheng, "Low sidelobe transmit antenna design for MIMO radar," *Chinese Journal of Radio Science*, vol. 27, pp. 1–6, 2012.

[23] H. He, P. Stoica, and J. Li, "Designing unimodular sequence sets with good correlations-including an

application to MIMO radar," *IEEE Transactions on Signal Processing*, vol. 57, pp. 4391–4405, 2009.

[24] J. A. Tropp, I. S. Dhillon, R. W. Heath, and T. Strohmer, "CDMA signature sequences with low peak-to-average-power ratio via alternating projection," in *Proceedings of Asilomar Conference on Signals, Systems and Computers*, 2003, pp. 475–479.

[25] J. A. Tropp, I. S. Dhillon, R. W. Heath, and T. Strohmer, "Designing structured tight frames via an alternating projection method," *IEEE Transactions on Information Theory*, vol. 51, pp. 188–209, 2005.

[26] A. Hassanien and S. Vorobyov, "Transmit energy focusing for DOA estimation in MIMO radar with collocated antennas," *IEEE Transactions on Signal Processing*, vol. 59, pp. 2669–2682, 2011.